Seismic reconstruction using a 3D tau-p transform

Maria S. Donati and Nicolas W. Martin

ABSTRACT

The present paper introduces a τ-p transform algorithm for 3D seismic data which not require any geometrical symmetry on the wavefield contained in the seismic data. It only requires to have the data regularly spaced. This algorithm express the τ-p transform by a four-fold sequence of 1D Fourier transforms in time, and spatial coordinates as indicated by McCowan and Brysk (1989) for a point source in an arbitrary medium.

In other words, the 3D τ-p transform is considered as an integration process of different two-dimensional τ-p transforms, each one representing a particular picture of the propagating wave field, along inline and crossline directions. The two-dimensional τ-p transform (back and forward) is performed in the k-w domain using the algorithm published by Wade and Gardner (1988) and Gardner and Lu (1991) based on the "Fourier slice theorem" or "projection slice theorem" (Kak and Rosenfeld, 1982).

The 3D τ-p transform algorithm is tested on synthetic data simulating a shot acquired on an horizontally layered earth model. The results are shown for P and converted data using two different S/N ratios (free-noise and 15% of random noise) showing the robustness of the algorithm for recovering the original shot gathers in the presence of noise.

INTRODUCTION

The τ-p transform is an attempt to preserve the wavefield characteristics of the seismic data. A seismic section in the τ-p domain offers an alternative view in which all subsurface reflectors are illuminated by incident energy of a fixed ray parameter. One advantage of working in the τ-p domain is that we can study the different wave modes as function of their corresponding slowness values ($p=1/v$), where v is the propagation velocity. Then, the τ-p transform is an useful processing tool because it provides an increased separation between different seismic waves (i.e., multiples, ground-roll, P and S waves among others).

Given that there is minimal deterioration of the seismic data due to transform artifacts, a simplified interpretation of field records and better noise suppression can be obtained in the τ-p transform. This transformation has been world-wide used and well researched for two-dimensional seismic data recording during decades. For 3D data there are some mathematical developments and several approaches taking advantage of particular symmetries in the data (Evans, 1991).

THEORY

The application of slant stacking to decompose plane wavefields into their component waves is well documented (Chapman, 1978; Stoffa et al., 1981; Diebold and Stoffa, 1981 among others). Commonly, the slant stack is defined as:

$$\Psi(p,\tau) = \int_{-\infty}^{\infty} u(\tau + px, x)dx \qquad (1)$$

where $u(t,x)$ are the data at time, t, and horizontal range, x. In seismic field, $u(t,x)$ represents any two dimensional seismic data recorded as a function of traveltime, t, and source-receivers offset, x, as result of a point-source excitation. The variable $t=\tau+px$ represents a line in the x-t plane with slope p (or slowness, $1/v$) and vertical intercept time τ (Fig. 1). Conceptually, the slant stack represents a process that maps the summed amplitudes along a given line with slope p and intercept time τ in the x-t domain into a point in the τ-p domain (Fig. 1).

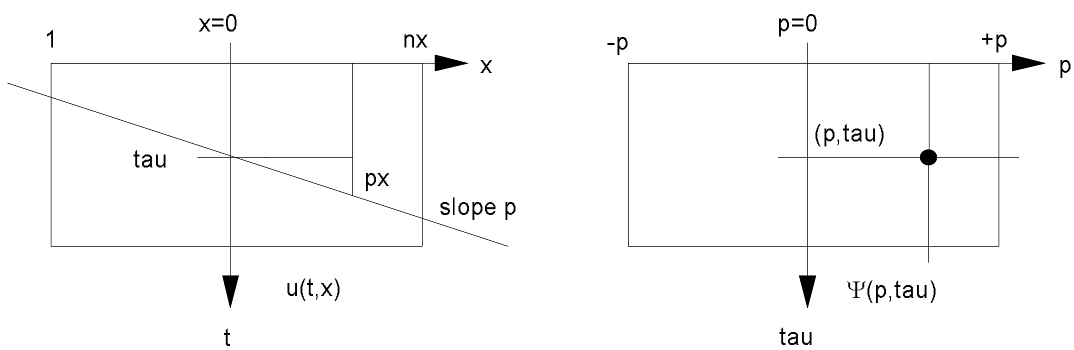

Fig. 1. The slant stack $\Psi(p, \tau)$ at any point (p, τ) is obtained by adding $u(x, t)$ along the line $t= \tau+px$. The value of the Ψ at the points where the line intersects each trace of u is obtained by interpolation (After Wade and Gardner, 1988).

In this way, summing amplitudes, of a given event, along lines with different p and τ values we can represent this event as an ellipse in the τ-p domain (Fig. 2).

The generalization of the slant stack to the 3D case is straightforward if we consider now that the slowness vector $\vec{p}$ has two components (p_x, p_y). Then, the 3D τ-p transform can be expressed for a point source acting at the origin of a uniform medium as follows:

$$\Psi(\tau, p_x, p_y) = \int_{-\infty}^{\infty} dx \int_{-\infty}^{\infty} u(\tau + p_x x + p_y y, x, y)dy \qquad (2)$$

where $u(t, x, y)$ represent the seismic data distributed over an areal coverage at time, t, without assuming any geometric symmetry (McCowan and Brysk, 1989; Chapman, 1981).

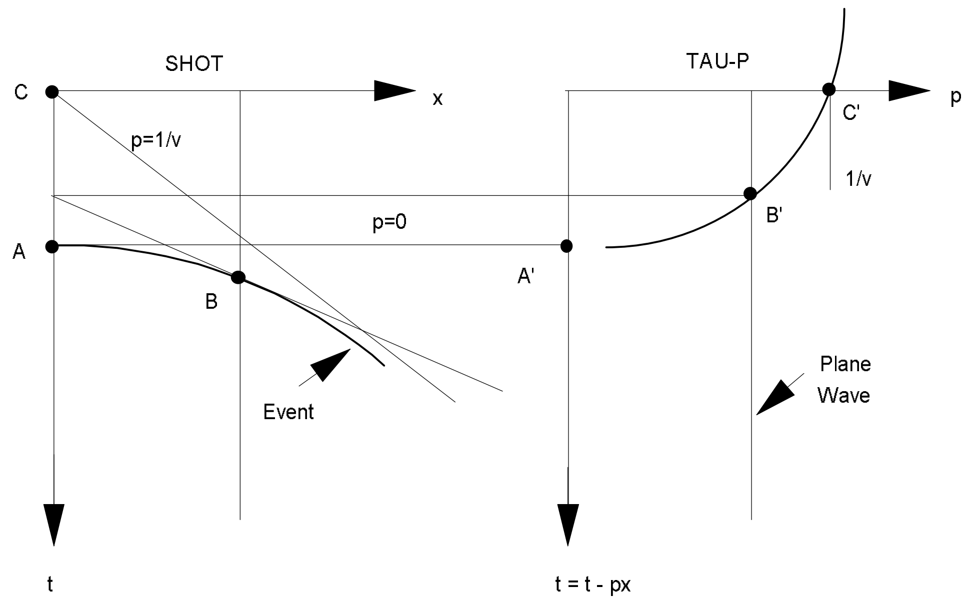

Fig. 2. A hyperbola on a shot gather maps onto an ellipse on the *p*-gather (After Yilmaz, 1987).

The reciprocal slat-stack operation for reconstructing (x, t) data from (p, τ) data is given by:

$$u(t,x,y,z) = -\frac{1}{4\pi^2}\frac{d^2}{dt^2}\int_{-\infty}^{\infty} dp_x \int_{-\infty}^{\infty} \Psi(t - p_x x - p_y y - qz, p_x, p_y)\, dp_y \qquad (3)$$

A more convenient way to express the 3D τ-p transform and its reciprocal s using direct and inverse Fourier transforms. In fact, the slant stack is reduced to a sequence of 1D Fourier transforms as follows:

$$\Psi(\tau, p_x, p_y) = \frac{1}{2\pi}\int_{-\infty}^{\infty} dw e^{-iw\tau}\int_{-\infty}^{\infty} dx e^{-iwp_x x}\int_{-\infty}^{\infty} dy e^{-iwp_y y}\int_{-\infty}^{\infty} dt e^{iwt} u(t,x,y) \qquad (4)$$

where w (=$2\pi f$) is the angular frequency. In the same way, the reciprocal operation is achieved by Fourier transforming back four times (McCowan and Brysk, 1989). The only consideration is that the transform variable for x is wp_x and y it is wp_y, so that an additional factor of w^2 appears during the operation $u(t, x, y)$ thus has the form:

$$u(t,x,y) = \frac{1}{8\pi^3}\int_{-\infty}^{\infty} dw e^{-iwt} w^2 \int_{-\infty}^{\infty} dp_x e^{iwp_x x}\int_{-\infty}^{\infty} dp_y e^{iwp_y y}\int_{-\infty}^{\infty} d\tau e^{iw\tau}\Psi(\tau, p_x, p_y) \qquad (5)$$

In other words, the slant stack can be performed either directly as a double integral over time-shifted traces (eq. (2)), or by a four-fold sequence of Fourier transforms (eq. (4)); so can its reciprocal, except for the differentiation (with reference to eq. (3) and (5)).

Then, for obtaining the τ-p transform we use the following procedure: i.) first, we convert the 3D input data from x-t domain to x-w domain (space-frequency domain) by direct Fourier transform, ii.) second, we pick out the volume along crossline direction and apply to each inline data a Fourier transform from x to wp_x, iii.) third, the last procedure is again apply on the data picked out from the (w, wp_x, y) volume along the inline direction performing a Fourier transform from y to wp_y, and iv.) fourth, we convert the resulting (w, wp_x, wp_y) volume using the inverse Fourier transform. All this sequence is performed shot by shot for all the inline and cross-line lines of each shot. Physically, with the inner three integrations in the last line of eq. (4), we expanded the propagating plane wave registered at the surface into component monofrequency plane waves and picked out the particular plane wave with a frequency w and a wavenumber with x and y components wp_x and wp_y. With the last integration in the same equation, we superpose a collection of such plane waves to build up a new wavelet following the criteria: They all have the same components of the Snell's parameter p_x and p_y; in other words, they all have the same direction of incidence into the medium, but different frequencies and wavenumbers. Hence, the slant stack represents a wavelet entering the medium with a specific orientation (McCowan and Brysk, 1989).

The inverse operation for recovering the original (t, x, y) volume is performed reversing the above sequence.

3D TAU-P TRANSFORM ALGORITHM

The process for obtaining the 3D τ-p transform as a sequence of Fourier transforms was implemented by modifying the forward and inverse 2D τ-p algorithms published by Gardner and Lu (1991). Both algorithms work in the k-w domain taking advantage of the "projection slice theorem" (Wade and Gardner, 1988). This theorem says that the 1D temporal coefficients of $\Psi(\tau, p)$ are identical to the coefficients in the 2D Fourier transform of $u(t, x)$ picked out long the radial line k=-pw, where k is the frequency corresponding to x and w, the frequency corresponding to t. The forward slant stack process is indicated in the Fig. 3a. Basically, it is used the fact that any radial line in the k-w domain is a column in the p-w domain. Conversely, any column in the k-w domain is a hyperbola in the p-w domain (Wade and Gardner, 1988). This last property let us reconstruct the (k, w) data from the (p, w) data by simply picking out values for k constant (along a hyperbola) as illustrated in Fig. 3b.

The extension for 3D data of these algorithms is indicated graphically in the Fig. 4. First, a (w, p_x, y) volume is obtained after applying the forward 2D τ-p transform in the k-w domain along the crossline direction. Second, the forward 2D τ-p transform is again applied along the inline direction(value of p_y constant) for obtaining the final

(w, p_x, p_y) volume. An inverse Fourier transform is applied on the resultant volume for reconstructing the original (t,x, y) data. For obtaining a 1:1 mapping, i.e., each coefficient for Ψ comes from a unique coefficient for u, it was applied a high-cut frequency filtering process for muting the (p, w) data outside the interval ($2\pi/w\mathrm{d}x$) for each frequency. The resulting (p, τ) slant stack contains enough information to recover the original $u(t, x, y)$ without aliasing.

SYNTHETIC MODELLING

For testing the 3D τ-p transform algorithm we generate a horizontally layered earth model with three flat homogeneous layers. Fig. 5 shows the depth model and the P wave velocities of each layer. This model was generated with the SIERRA modelling package. A single 3D a shot record was acquired on this synthetic model consist of 60 receivers distributed along six inline lines in the North-South direction and ten cross-line lines oriented East-West. The source was located at the left inferior corner of this patch (Fig. 6). The distance between inline and crossline lines was kept fixed at 75 m, respectively.

Four different experiments were performed for evaluating the algorithm in reconstructing the original wavefield under free-noise and noisy conditions. These experiments are described as follows.

Experiment 1

It represents a synthetic 3D P-P shot record of the three flat horizons of the depth model (Fig. 7a). The reconstructed shot record is indicated in the figure 7b for 50 values of slowness, p (50 for p_x and 50 for p_y). It represents a p increment of 0.0000134 s/m with a range of p values between 0 - 0.00067 s/m equivalent to a minimum P wave velocity of 1500 m/s for both inline and crossline directions. It is obvious the good performance of the algorithm during the reconstruction of the input shot. Some noise is left on the record after applying the algorithm. Fig. 7c shows the result of the reconstruction increasing the total number of p values by a factor of 2. The remnant noise was practically eliminated. It indicates that a more fine sampling in the slowness p let us obtain a better wavefield reconstruction. The correspondent representation of the original shot record in the τ-p transform is indicated in the Fig. 7d. The short spread used in the acquisition produces linear noise interfering with the ellipses associated to the events. In fact, as indicated by Phinney et al. (1981) slant stacks of lines for finite-length discrete data do not transform exactly into points regardless of the method used for obtaining the direct and inverse τ-p transform.

Experiment 2

In this case it was added a 15 percent of random noise on the 3D P-P shot record (Fig. 8a). We can see the reflections associated with the first and second flat reflectors but the reflection from the last one is masked by the noise background. The reconstructed shot record (Fig. 8b), using the same spacing between *p* traces in the *τ-p* domain shown in experiment 1, shows an excellent recovering of the three events in presence of noise. Although, the amplitudes of the events are diminished after the reconstruction is possible to identify the two upper *P* wave events. The last event associated with the deepest layer have been recovered too but it is partially masked by the noise.

Experiment 3

The goal of this experiment is evaluate the reconstruction of a shot record containing converted waves (Fig. 9a). The reconstructed record is indicated in the figure 9b. gain, the reconstruction of the *P-P* and *P-SV* waves is very good but noisy. Here, the reflections associated with the converted waves appear with less amplitude due to superposition of the *P* and *SV* energies in the *τ-p* domain as consequence of the finite-length or short offset of the spread in the *x-t* domain. As the energy associated with the *P*-wave is stronger than the *SV*-wave energy; it masks partially the *SV* events specially those arriving at longer traveltime.

Experiment 4

The effect of the random noise on the reconstruction of the 3C converted wave records is considered (Fig. 10a) where the noise level is kept at 15 percent as experiment 2. The result is shown in the Fig. 10b. It is obvious that 3D *τ-p* transform fails to recover the *SV* wave events due to its energy is less than the noise present in the data. The reconstruction of the *SV* waves is effected by the *P-P* and *P-S*V interference and the low S/N ratio. The *P*-wave energy is more coherent in the *τ-p* domain and it permits a better performance of the algorithm.

CONCLUSIONS

1) It has been presented a 3D *τ-p* transform which not requires to assume any geometric symmetry in the wavefield contained in the seismic data.

2) This 3D *τ-p* transform (forward and inverse)works in the *k-w* domain by expressing the slant stack process as a four-fold sequence of Fourier transforms which convert the (t, x, y) data to (w, wp_x, wp_y) data. This is a trade-off for the expense disk space required for performing the necessary Fourier transforms, but these are typically very fast and eliminate the problem of double summation of the seismic amplitudes along (p_x, p_y) planes as would be assumed for an implementation of Stoffa's method for 3D data.

3.) The preliminary results of the application of the 3D *τ-p* transform on synthetic 3D shot records, containing *P* and converted waves with different S/N ratios (free-noise and 15% random noise), show its robustness for recovering the initial wavefield in real field conditions. Any ulterior noise-elimination algorithm during processing will increase the reconstruction capacity of the 3D τ-p transform algorithm.

ACKNOWLEDGMENTS

We wish to thank the sponsors of the CREWES Project at the University of Calgary for their support of this study.

REFERENCES

Chapman, C.H., 1978, A new method for computing synthetic seismograms: Geophy. J. Roy. Astr. Soc., v. 54, p. 481-518.

Chapman, C.H., 1981, Generalized radon transforms and slant stacks: Geophy. J. Roy. Astr. Soc., v. 66, p. 445-453.

Evans, B., 1991, ET- a slant-stack transform of three dimensional data: Expl. Geophy., v. 22, p. 135-142.

Diebold, J.B. and Stoffa, P.L., 1981, The traveltime equation, tau-p mapping and inversion common midpoint data: Geophysics, v. 46, p. 238-254.

Kak, .C. and Rosenfield, A. 1982, Digital picture processing -Volume 1: Academic Press, Inc.

McCowan, D.W.and Brysk, H.,1989, Cartesian and cylindrical slant stacks, Paul L. Stoffa (ed.), Tau-p: A Plane Wave Approach to the Analysis of Seismic Data, p. 1-33.

Pan, N.D. and Gardner, G.H.F., 1984, Forward and inverse p-tau transformations using k-f transforms: Seismic Acoustics Laboratory Semi- Annual Progress Review, 14, 241-270.

Phinney, R.A., Chowdhury, K.R., and Frazer, L.N., 1981, Transformation and analysis of record sections: J. Geoph. Res., 86, 359-377. Tatham, R.H., 1984, Multidimensional filtering of seismic data: Proceedings of the IEEE, 72, No. 10, Oct.

Stoffa, P.L., Buhl, P., Diebold, J.B., and Wenzel, F., 1981, Direct mapping of seismic data to the domain of intercept time and ray parameter: Geophysics, V.46, p. 233-267.

Wade, J.C. and Gardner, G.H.F.,1988, Slant-stack inversion by hyperbolae extraction in the Fourier domain: 58th Ann. Internat. Mtg., Soc. Expl. Geophys., Expanded Abstracts, p. 676-679..

Wade, J.C. and Lu, L., 1991, Some fundamentals of slant-stack methods: Slant-stack processing, SEG (Appendix 1), p. 457-481.

Yilmaz, O., Seismic data processing, 1987: SEG.

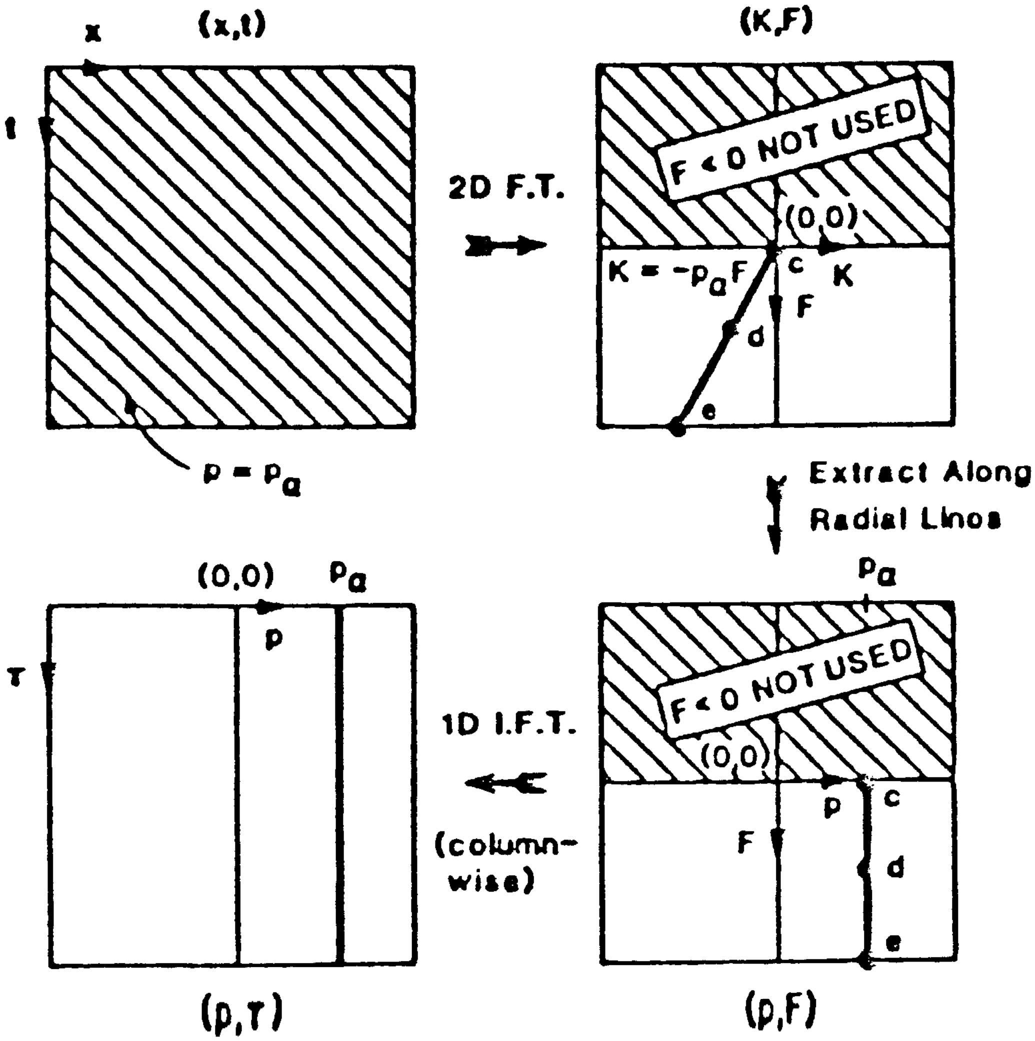

Fig. 3a. Scheme for constructing slant stack with 2D Fourier transforms (After Wade and Gardner, 1988).

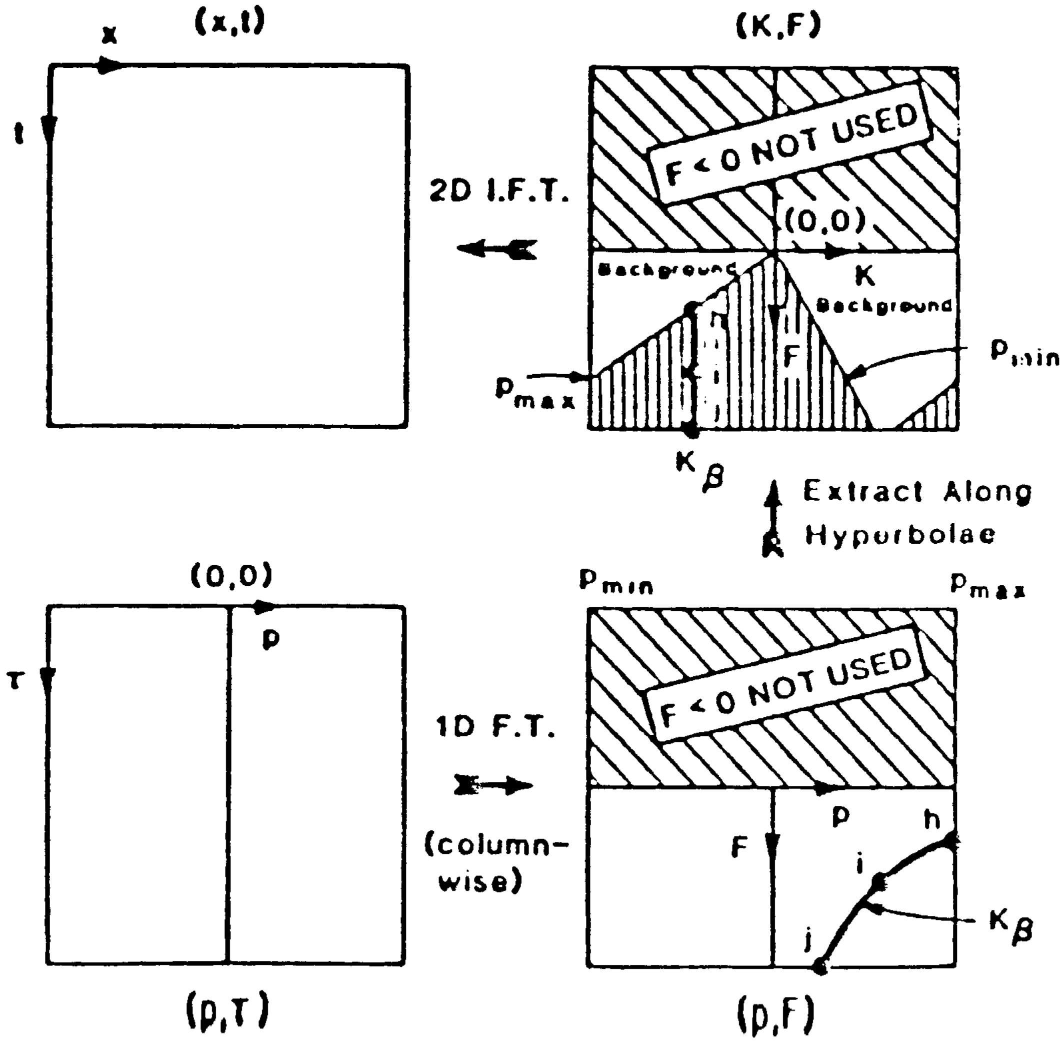

Fig. 3b. Scheme for reconstructing (t,x) data from (τ, p) data with 2D Fourier transforms (After Wade and Gardner, 1988).

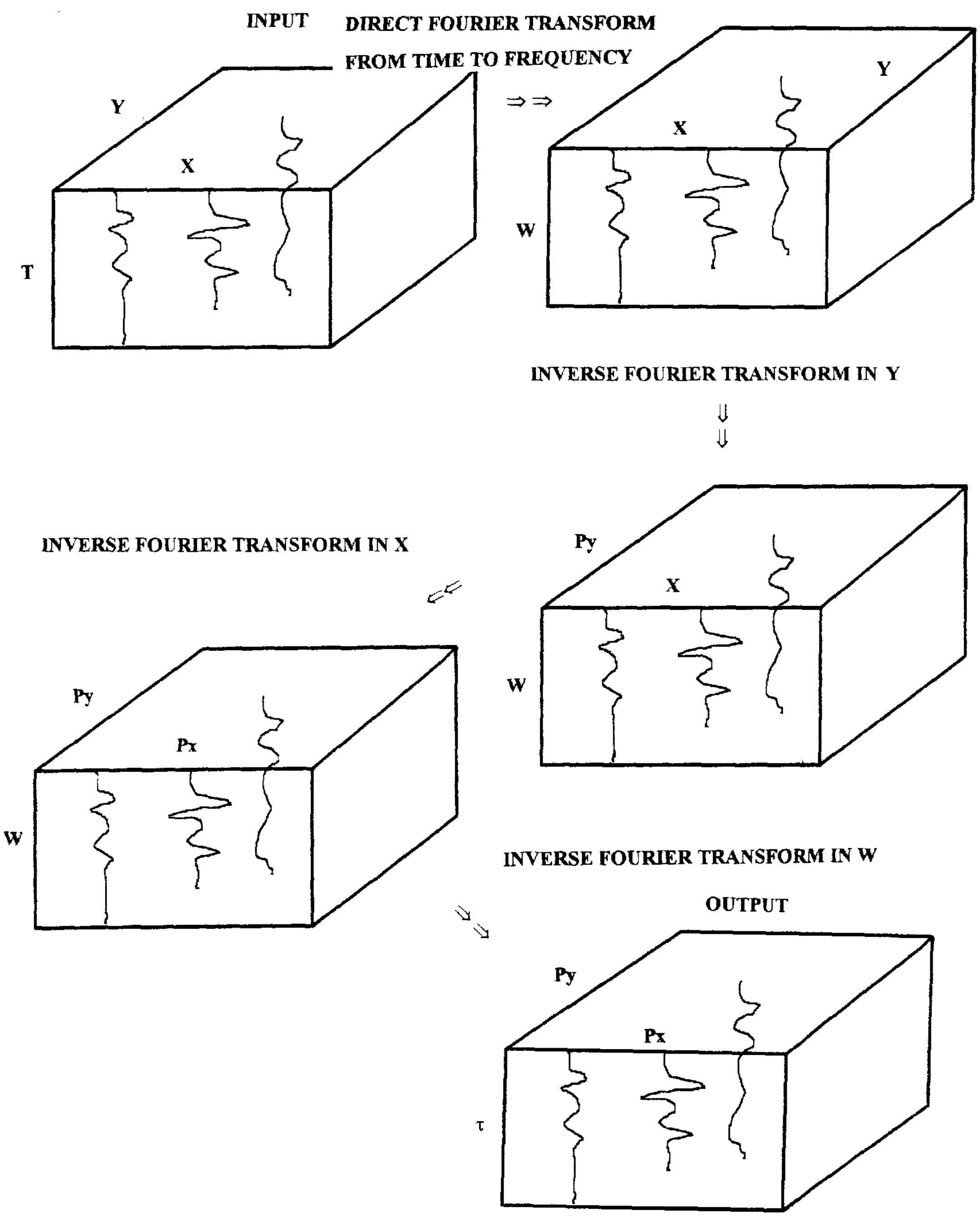

Fig. 4. Schematic view of 3D τ-p transform applied on data distributed over an areal coverage without assuming any geometric symmetry.

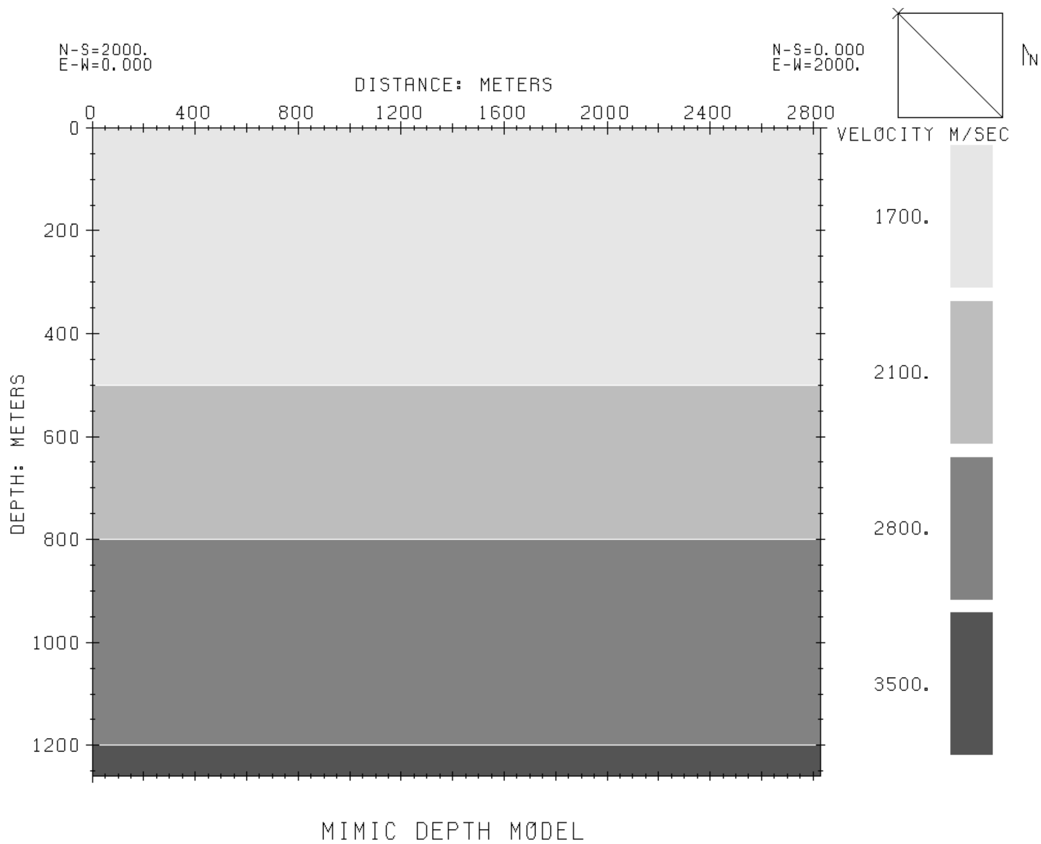

Fig. 5. Depth model representing a horizontally layered earth with constant *P* and *S* wave velocities.

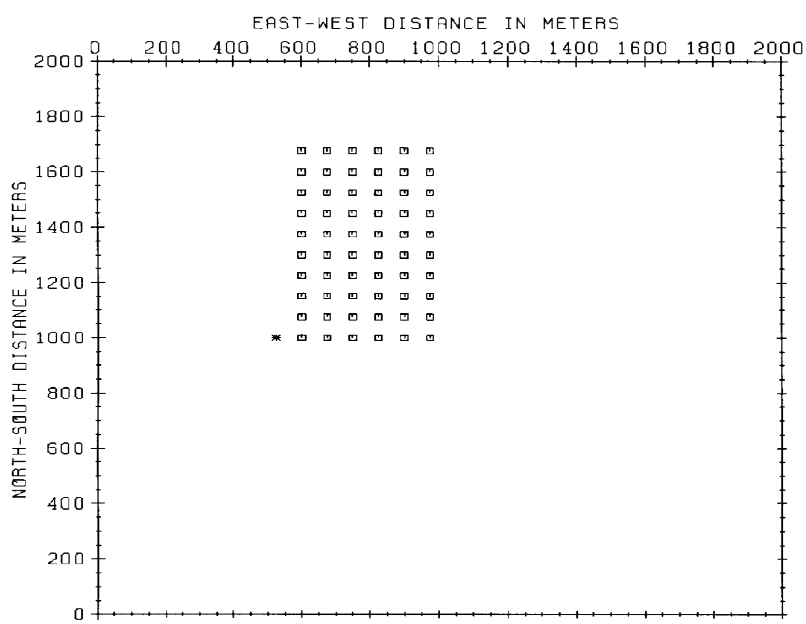

Fig. 6. Acquisition geometry for a 3D shot record. The inlines are oriented along the North-South direction and the crosslines along the East-West direction. The source is represented by the simbol (*) and the receivers by (□) on this display.

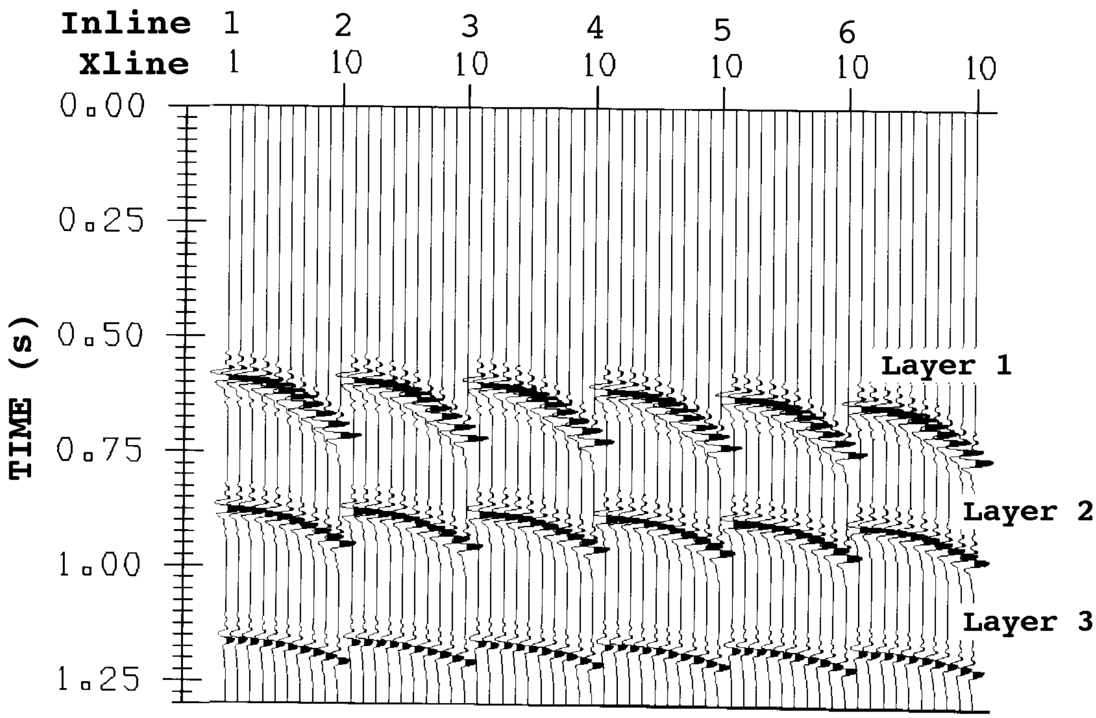

Fig. 7. (a) The input 3D shot record showing the *P-P* arrivals.

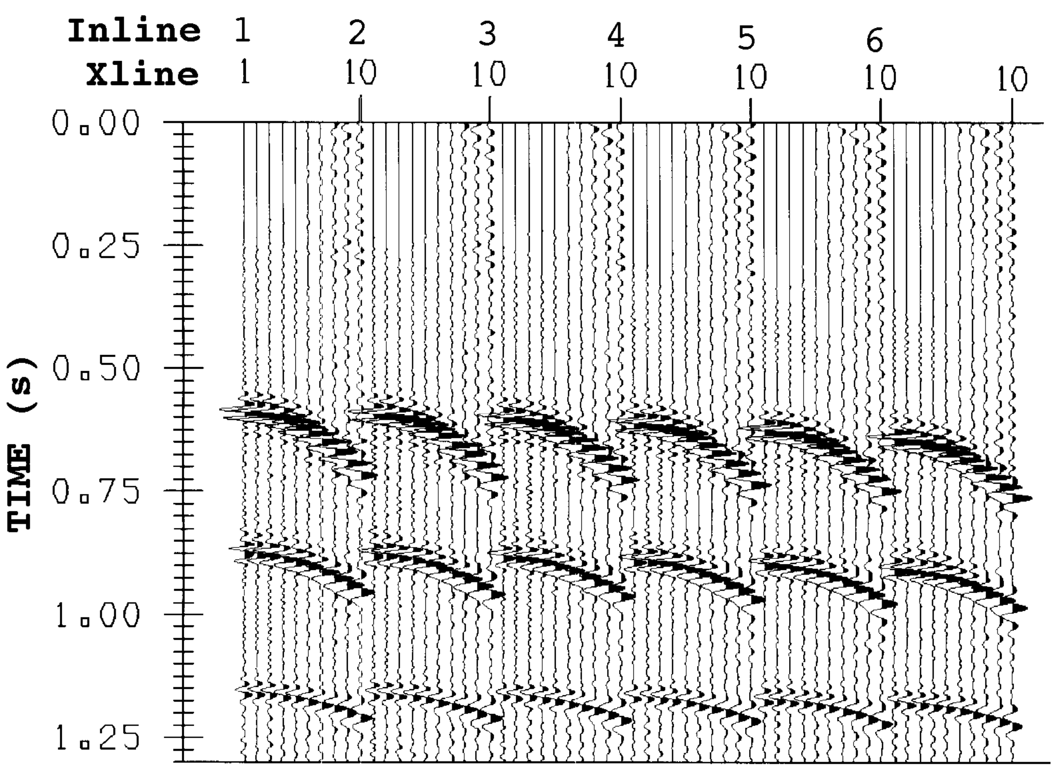

Fig. 7. (b) Reconstruction after applying the 3D τ-p transform considering 50 slowness values in each x and y direction.

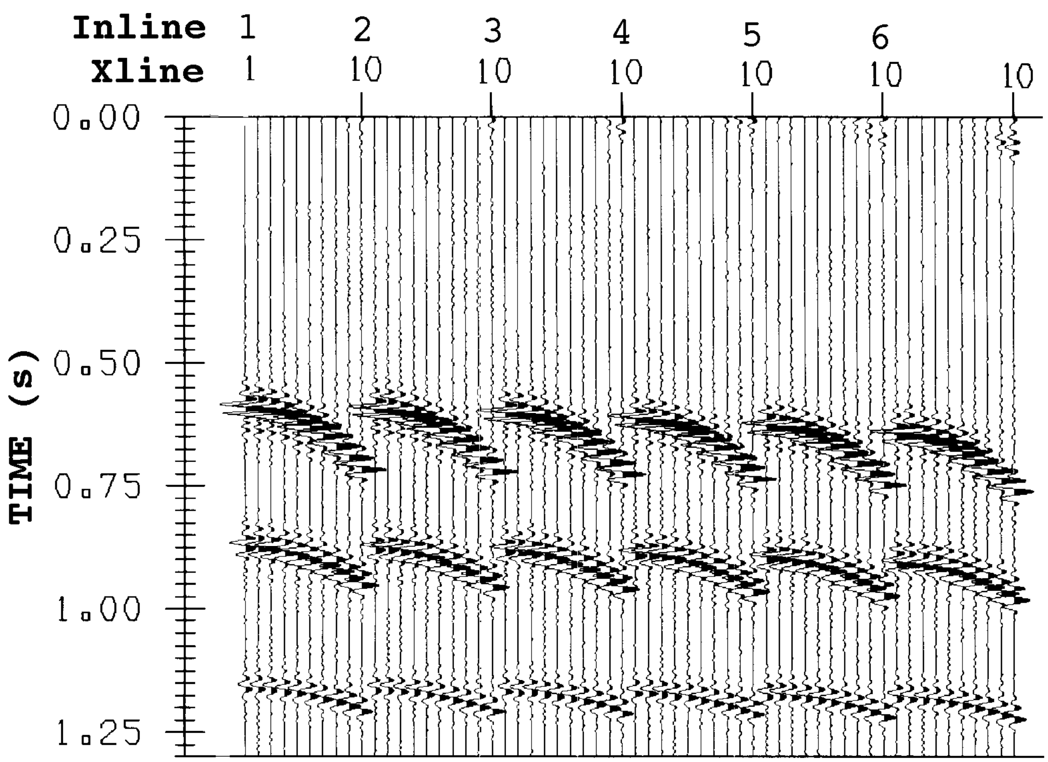

Fig. 7c. The reconstructed 3D shot record after applying the 3D τ-p transform considering 100 slowness values in each x and y direction.

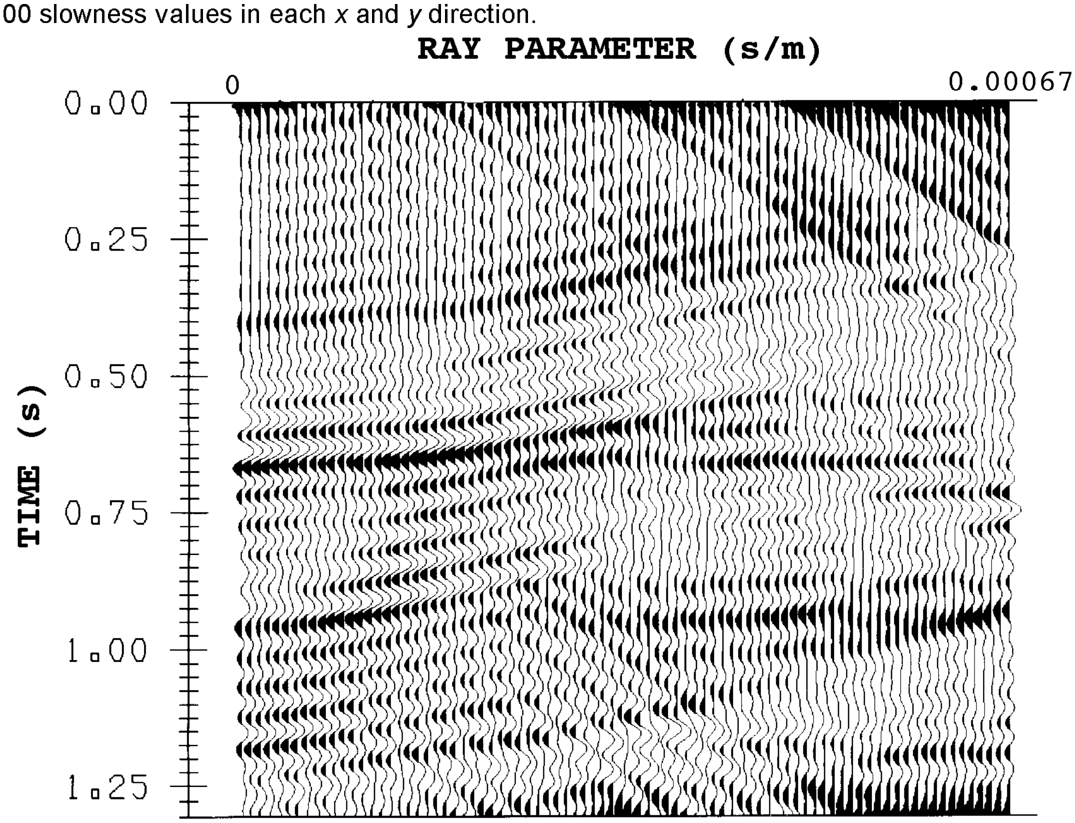

Fig. 7d. The representation of the 3D shot record for the inline number 1 in the τ-p domain.

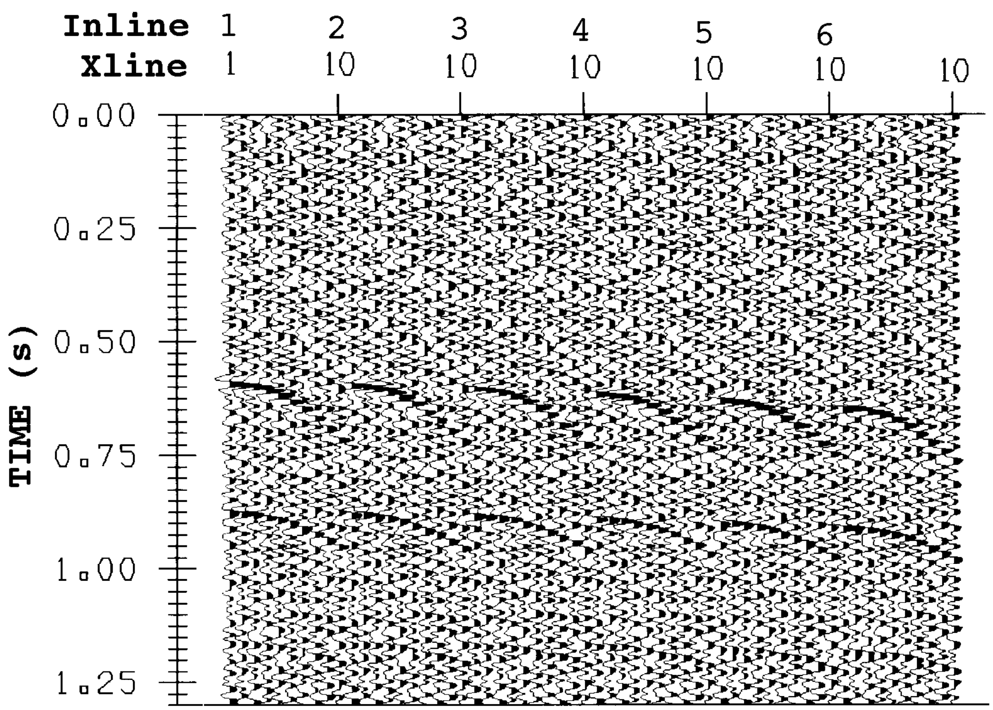

Fig. 8a. The input 3D shot record showing the *P-P* arrivals, with 15% of background noise, for the three flat layers in the depth model shown in Fig. 5.

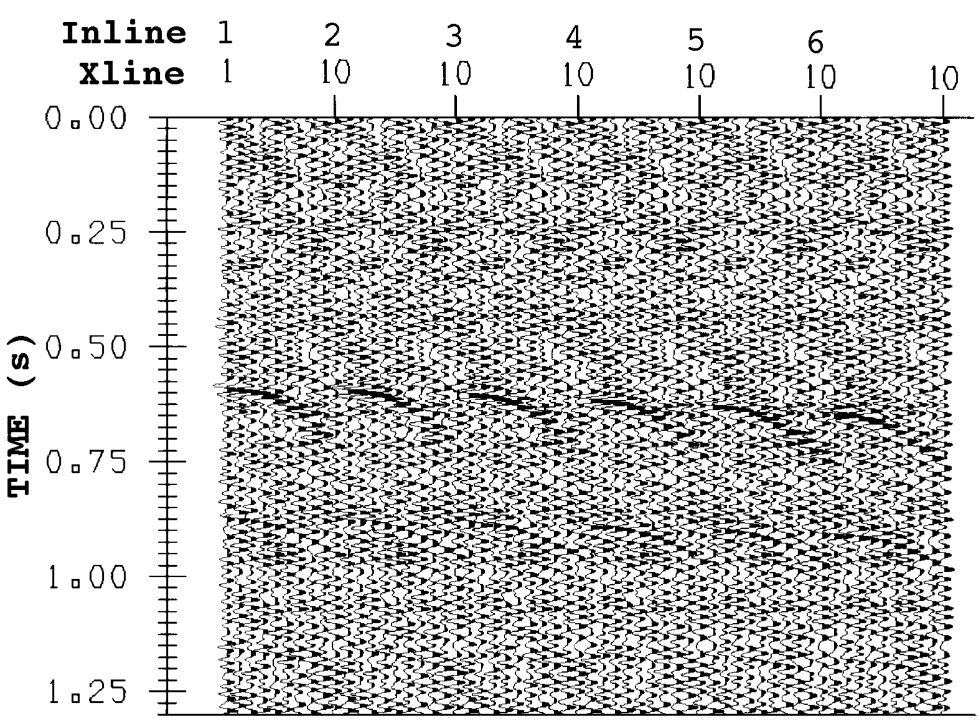

Fig. 8b. The reconstructed 3D shot record, shown in Fig. 8a, after applying the 3D τ-*p* transform in the presence of noise.

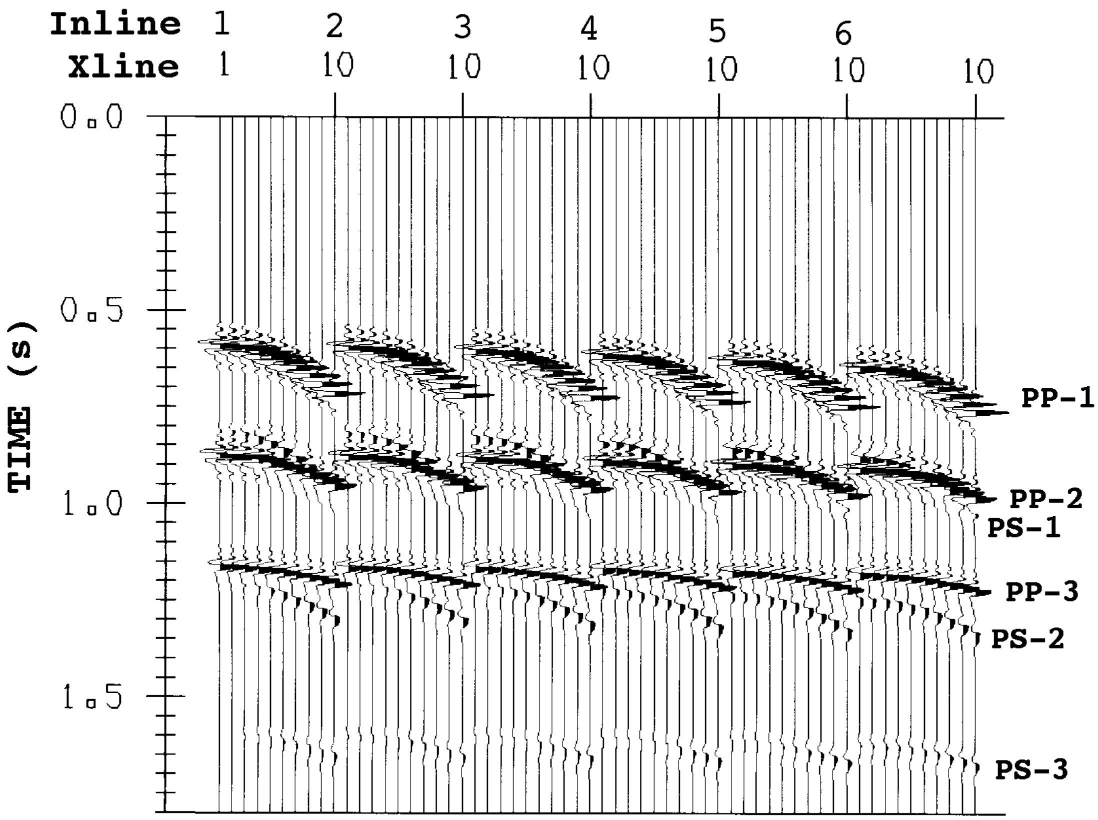

Fig. 9a. The input 3D shot record showing the *P-P* and *P-SV* arrivals (free-noise condition).

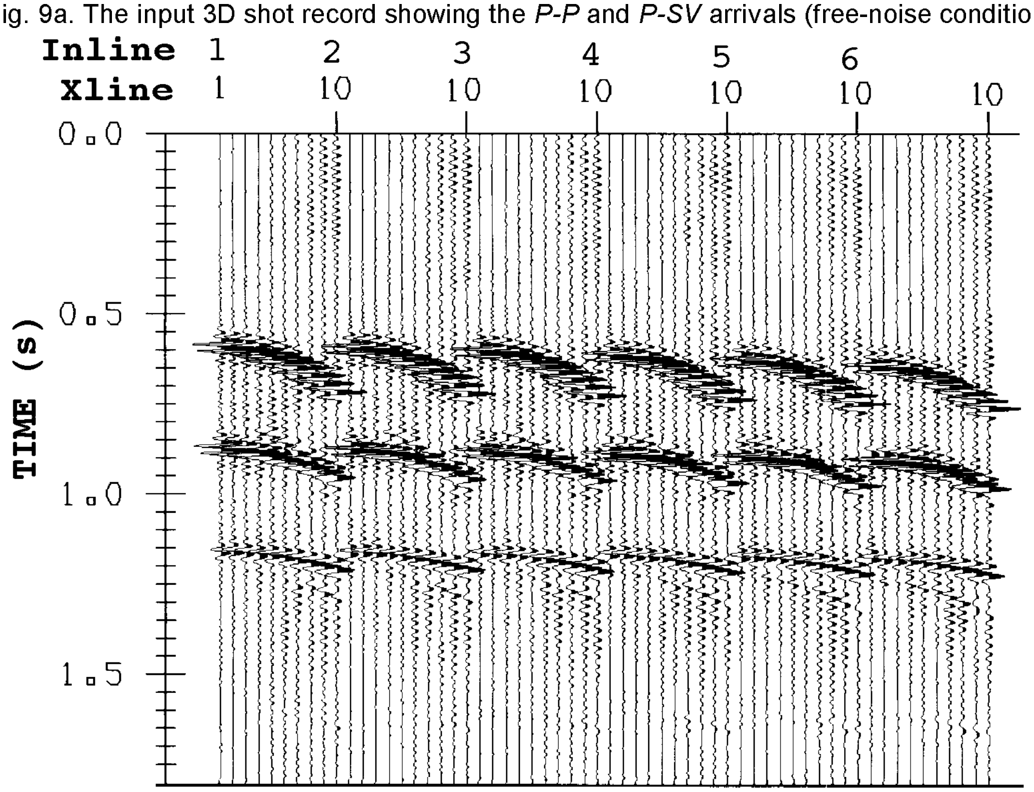

Fig. 9b. The reconstructed 3D shot record after applying the 3D τ-*p* transform.

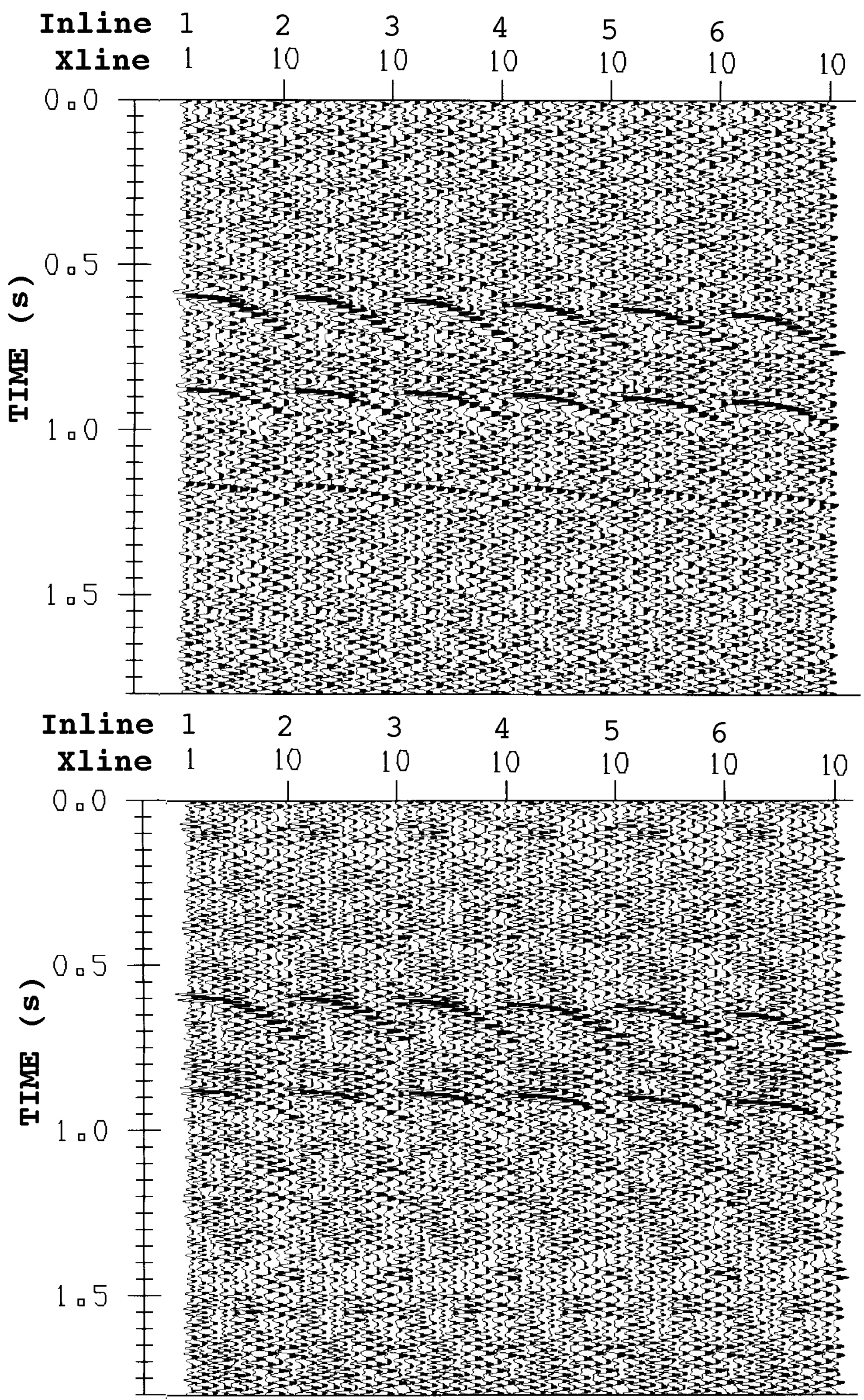

Fig.10. (a) 3D shot for converted waves (top), (b) Reconstructed data (bottom).